JOURNAL OF MAGNETIC RESONANCE **126,** 213–220 (1997)
ARTICLE NO. MN971175

Fracture Characterization with NMR Spectroscopic Techniques

C. T. Philip Chang, Jinli Qiao,* Songhua Chen,† and A. Ted Watson

Department of Chemical Engineering, Texas A&M University, College Station, Texas 77843-3122

Received October 31, 1996; revised April 7, 1997

Determination of suitable techniques and analyses that can be implemented by NMR well logging can greatly improve the characterization of underground petroleum reservoirs and aquifers. In this paper, the feasibility for using various NMR methods for detection and characterization of fractures is explored. Analyses of experimental data obtained with a variety of samples are presented. It is shown that relaxation contrasts are useful for separating the signal contributions from fluids in the fractures and the porous matrix, and that relaxation weighting can be used in combination with other NMR techniques for enhancing fracture characterization.

INTRODUCTION

It is necessary to characterize underground porous rock formations and the fluids they contain in order to make effective decisions regarding the production from petroleum reservoirs, as well as the utilization and remediation of groundwater resources. Given the relative inaccessibility of these formations, characterization remains a very difficult task. Well logging is commonly used, whereby a variety of different properties, such as resistivity and acoustics, are measured in the formations. Those measurements are in turn used to estimate petrophysical properties, such as porosities and fluid saturations, which are important for assessing the amount and mobility of the fluids.

Recent developments have led to the commercial applications of nuclear magnetic resonance to well logging (*1*). The versatility of NMR measurements to molecular events provides a great potential for its use to characterize reservoir formations. Currently, the primary NMR technique implemented on logging tools is CPMG measurements, from which estimates of porosity, fluid saturations, and permeabilities are made. Other techniques can be implemented with modifications in current software and hardware designs. It is important to assess the value that other techniques may have for characterizing reservoir properties in order to motivate and lead hardware and software development. Here we investigate the feasibility for detecting and characterizing fractures by NMR spectroscopic measurements.

Fractures are necessary for economical production of petroleum from many low permeability reservoirs. The characterization of fractures and microfractures is highly desirable since it can provide valuable information for assessing reservoir producibility or monitoring fracture treatments or other methods for enhancing production. It is generally true that no conventional tool has the capability for direct observation of fluids in fractures which can be used to characterize fractures or fissures. We believe NMR techniques have the potential to provide that information.

Investigations of the use of NMR imaging techniques for characterizing fractures and fluid distributions in fractures have been reported previously (*2, 3*). The imaging techniques are effective for characterizing fractures and studying flow in fractured systems in laboratory measurements. However, it would be difficult to implement these techniques with NMR logging tools due to hardware and logging time constraints. Spectroscopic techniques which can be interpreted to reveal fractures are more useful for NMR logging applications.

The use of spectroscopic techniques for fracture characterization is particularly challenging because the information obtained from spectroscopic measurements represents a mixture of signals from fluids in the porous matrix and fracture regions. In addition, in many fractured systems, the volume of the fracture represents only a small fraction of the total pore volume of the entire sample, so it can be difficult to separate the weak NMR signal corresponding to fluids in the fractures from the signal corresponding to the fluids in the porous matrix.

In this paper, we investigate T_2 relaxation distributions, lineshapes, and T_2-weighting techniques for characterizing fluid distributions in fractured systems. The advantages and disadvantages of these techniques are discussed.

BACKGROUND AND THEORY

Lineshape Analysis in Fractured Systems

Inhomogeneous line broadening in porous media arises from the internal field gradients due to the fluid–solid in-

* Now at Syntron, Inc.
† Now at Western Atlas Logging Service.

1090-7807/97 $25.00

terfacial heterogeneities, and pore-structural and rock-compositional heterogeneities. For porous media characteristic of petroleum reservoirs, the line broadening can be severe due to appreciable concentrations of magnetic impurities. While the line broadening can limit certain analyses, linewidths and lineshapes do contain pore geometry information which could be useful for characterizing porous media. In particular, in situations for which the pore structure is the dominant contributor to line broadening, such as in fractured systems, the use of lineshape analysis provides certain advantages.

Durney *et al.* (*4*) found that, for structurally heterogeneous porous systems, NMR lines are both broadened and shifted from their corresponding bulk fluid resonance frequencies. They have calculated the lineshift in simplified geometries and observed lineshifts experimentally using structurally heterogeneous phantoms and porous media characteristic of biological samples. No linewidth studies have been reported for analysis of pore structures in porous rock.

The presence of fractures in porous media can result in significantly broadened lineshapes since resonance frequencies corresponding to the fractures and porous matrix are shifted by different amounts. Specifically, the part of the spectrum corresponding to the fracture is narrower, and it is shifted from the bulk fluid resonance frequency by a smaller amount than the part of the spectrum corresponding to the porous matrix. Thus, the observed spectrum, which is a combination of the two parts of the signals, can be expressed as

$$M(\omega) = \sum_{i=1}^{2} M_{0i}\, f_i(\omega - \omega_{0i}), \qquad [1]$$

where i refers to either the fluid in the fractures or the porous matrix, M_{0i} is the peak magnitude, ω_{0i} is the position of the peak on the spectrum, and $f_i(\omega - \omega_{0i})$ is the lineshape function. The lineshift between the fluid in the fractures and the porous matrix can be defined as

$$\Delta\omega = \omega_{01} - \omega_{02}. \qquad [2]$$

The lineshape corresponding to each part of the spectrum can be approximated by either a Lorentzian lineshape,

$$f_i(\omega) = \frac{1/\delta\omega_i}{1 + (\omega - \omega_{0i})^2/(\delta\omega_i)^2}, \qquad [3]$$

where $\delta\omega_i$ corresponds to $1/T_2^*$, or a Gaussian lineshape,

$$f_i(\omega) = \exp\left[-\frac{(\omega - \omega_{0i})^2}{2\sigma_i^2}\right], \qquad [4]$$

where σ_i is the variance of the line.

Because of inhomogeneous line broadening, the two parts of the spectrum usually overlap. The two separate parts of the spectrum can be estimated using nonlinear regression. In this study, we represent the measured response using the model

$$M(\omega_j) = \sum_{i=1}^{2} M_{0i}\, f_i(\omega_j - \omega_{0i}) + a + b\omega_j. \qquad [5]$$

The lineshape functions are represented by either Eq. [3] or [4], and a and b are the zeroth-order (constant) and first-order (linear) baseline corrections, respectively. The parameters within the model are estimated by minimizing the sum of squared residuals

$$\mathrm{RSS} = \sum_{j=1}^{m} [M(\omega_j) - M^{\mathrm{obs}}(\omega_j)]^2, \qquad [6]$$

where $M^{\mathrm{obs}}(\omega_j)$ is a measured value. In our work, the Lorentzian lineshape provided a more precise fit than the Gaussian lineshape. In the Lorentzian lineshape model, eight fitting parameters are used (a, b, M_{01}, M_{02}, ω_{01}, ω_{02}, $\delta\omega_1$, and $\delta\omega_2$).

Identifying Fractures from T_2 Distribution Analysis

It has been demonstrated that relaxation time differences for fluid in fractures and in the porous matrix can be utilized to distinguish fractures from the porous matrix using MRI (*2*). In that work, different inversion times in the inversion-recovery spin-echo imaging sequence were used to selectively nullify signals from either fluids in the fractures or the porous matrix. Although this particular technique may not be directly useful for spectroscopic characterization of fractures, the idea of utilizing relaxation contrasts between the porous matrix and fractures is useful. Among the various relaxation measurement techniques, those measuring T_2 may be the most effective for fracture identification.

Under the fast exchange approximation, the dependence of relaxation time on the surface-to-volume ratio for a pore can be expressed as (*5*)

$$\frac{1}{T_i} = \frac{1}{T_{ib}} + \frac{\lambda}{T_{is}}\frac{S_p}{V_p}, \qquad [7]$$

where $i = 1, 2$, for longitudinal or transverse relaxation. The measured magnetization decay represents a convolution of the relaxation of fluids in the various pores (*6*). Consider now the relaxation of fluid in fractures. If fractures are sufficiently narrow so that Eq. [7] is valid, we can expect that the relaxation rate will be proportional to the width, w, of the fracture since

$$\frac{V}{S} = w. \qquad [8]$$

Even in the case of broad fractures where the fast-diffusion approximation may not be valid, we expect a similar trend, with the relaxation time for the fluid in the fractures approaching that for the bulk fluid as the fracture width increases.

The ability to detect fractures depends on the V/S ratio of the fractures being different from those values within the porous matrix. The following discussion indicates that this may be the case in many systems. For simplicity, we take a spherical pore geometry. To obtain the same value of V/S for the two regions, it would require that $w = 6d$, where d is the diameter of the pore. For example, a fracture of width 200 μm has the same value of V/S as a 1.2 mm diameter pore. We expect that many media will tend to have fractures as large, or larger, while exhibiting few, if any, pores of that size; thus, the identification of fractures from T_2 distributions should be possible.

Identifying Fractures with T_2-Weighting Techniques

Since relaxation decay in the porous matrix is much faster than in the fracture, different lineshapes will be observed corresponding to different TE values. Thus, measurements using different TE values may be useful to probe fractured media.

The magnetization for the T_2-weighted spectra can be expressed as

$$M(\omega, \mathrm{TE}) = \sum_{k_\mathrm{f}}^{N_\mathrm{f}} M_{0\mathrm{f}} \exp(-\mathrm{TE}/T_{2k_\mathrm{f}})\, f_\mathrm{f}(\omega_{0\mathrm{f}}) + \sum_{k_\mathrm{m}}^{N_\mathrm{m}} M_{0\mathrm{m}} \exp(-\mathrm{TE}/T_{2k_\mathrm{m}})\, f_\mathrm{m}(\omega_{0\mathrm{m}}), \quad [9]$$

where the first term corresponds to the contribution from fluid in fractures and the second term from fluid in porous matrix. For fluid in fractures, $N_\mathrm{f} = 1$ is approximately valid for a single fracture with uniform width but would be greater than one if multiple fractures with different widths, or a single fracture with considerable variation in width, were present. If the TE value is sufficiently long such that $\exp(-\mathrm{TE}/T_{2k_\mathrm{m}}) \approx 0$ for the longest k_m component, but is not so long so that $\exp(-\mathrm{TE}/T_{2k_\mathrm{f}})$ is not fully decayed, the observed lineshape will represent fluid in the fractures only. By comparing the lineshapes obtained at long TE values with those at TE $\approx$ 0, one can separate the contributions from the different regions—fracture and matrix—even for cases where the two parts of the line are overlapping in the spectra corresponding to short TE values.

RESULTS AND DISCUSSION

All NMR measurements were performed in a GE 2-T CSI system with a 4.45 cm i.d. birdcage RF coil. Spin-echo sequences were used to obtain relaxation and lineshape data. Two-dimensional cross-sectional spin-echo images were used to verify the fracture widths.

Low permeability Leuters and Calico limestone samples were used. Artificial fractures were made in the rock samples, and the widths of the fractures were controlled by inserting different-sized glass beads. Fractures were sealed with epoxy on the sides. Samples were saturated with either water or hexadecane.

Lineshape Analysis with Relaxation-Weighted Data

The first set of the experiments were performed in four water-saturated Leuters limestone samples cored from a single block of rock. Three of the samples had an artificial fracture, each differing in the fracture width, and the fourth sample had no fracture. Two-dimensional spin-density images were used for examining the widths of fractures in the three samples with fractures. From these images, the widths of the fractures are estimated to be approximately $w = 0.2$, 0.35, and 0.75 mm, respectively. The actual fracture widths are not expected to be significantly different from those val-

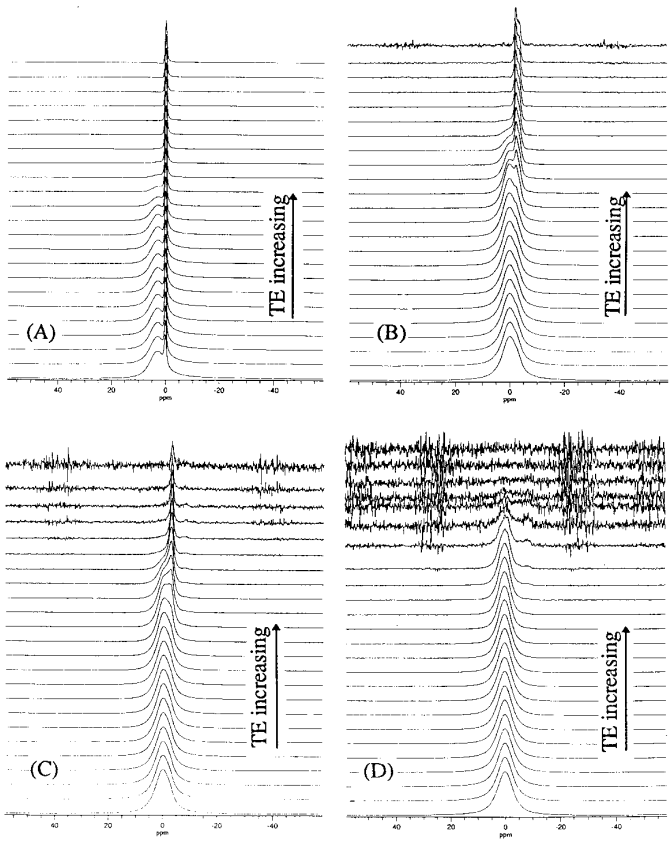

FIG. 1. Composite plot of lineshapes (magnitudes rescaled) as a function of echo times for water-saturated Leuters limestone samples with different fracture widths: (A) wide, (B) middle width, (C) narrow, and (D) no fracture. The echo time increases from 0.1 to 200 ms (bottom to top).

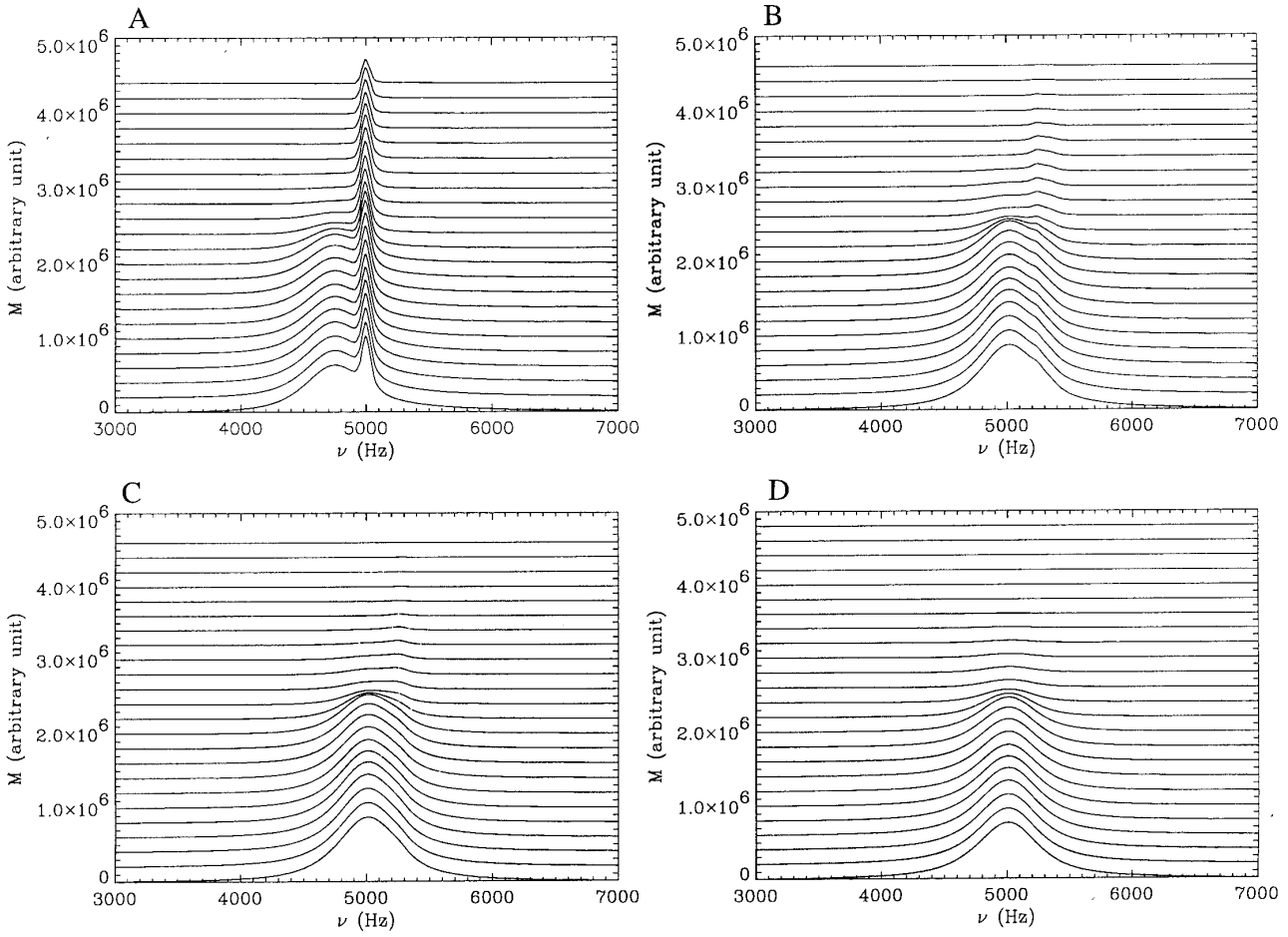

FIG. 2. Same as described in the legend to Fig. 1 except magnitudes were not rescaled.

ues, although small uncertainties may occur due to a slight alignment problem between the gradient of the fracture plane and due to linewidth limitations (*2*).

Figures 1A–1D show the lineshapes measured from the four samples. The multiple spectra shown in each figure represent data taken with different echo times TE ranging from 0.1 to 200 ms. The spectra are plotted in the order of their corresponding experimental echo times TE which increase from the bottom to the top of each figure. The intensities of the spectra on each figure were rescaled according to the maximum intensity of each spectrum so that the relatively slower-decaying signals of the fluid in the fracture, corresponding to data taken with long TE values, can be readily visualized. As a comparison, the unscaled spectra corresponding to Figs. 1A–1D are plotted in Figs. 2A–2D.

Several interesting features can be observed from these figures. First, for the sample with no fracture, a broad single-peaked lineshape (Fig. 1D) was observed for the spectra of all the TE values. In contrast, for the sample with a wide fracture (Fig. 1A), distinguishable dual-peak lineshapes are observed for spectra obtained with short echo times. Since the signal corresponding to the fluid in the porous matrix decays much faster than that corresponding to the fluid in the fracture, that part of the spectra was not observed at longer TE values. Consequently, only a single peak with relatively narrow linewidth, representing fluid in the fracture, was observed.

The two peaks shown in the spectra of Fig. 1A, although still overlapping, are fairly distinguishable. On the other hand, overlapping of the fracture signal and the porous matrix signal occurs more severely for the cases with narrower fractures because of the weaker signal due to the lower total fluid volumes in the fractures. Figure 1C shows the spectra of the sample with the narrowest fracture; only single-peaked lineshapes are observed for short TE values, which appear similar to the sample with no fracture. For those cases, it would be difficult to identify the fracture from spectra measured using a short TE value. However, the fracture can be identified by observing the trends with TE. For all three cases, significant signal from the fluid in the matrix is observed with small TE values. As TE increases, the signal

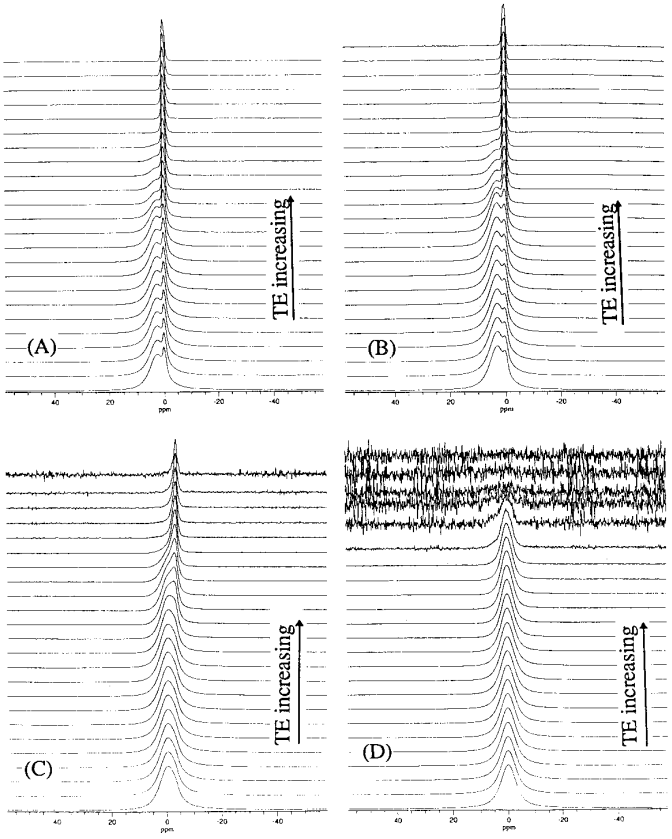

FIG. 3. Lineshapes (magnitudes rescaled) as a function of echo times, ranging from 0.1 to 200 ms (bottom to top), for oil-saturated Leuters limestone samples with different fracture widths: (A) wide, (B) middle width, (C) narrow, and (D) no fracture.

from the matrix region decreases, due to its greater relaxation rate. The signal from the fracture region, which is narrower and is shifted to the right, becomes more apparent as TE increases.

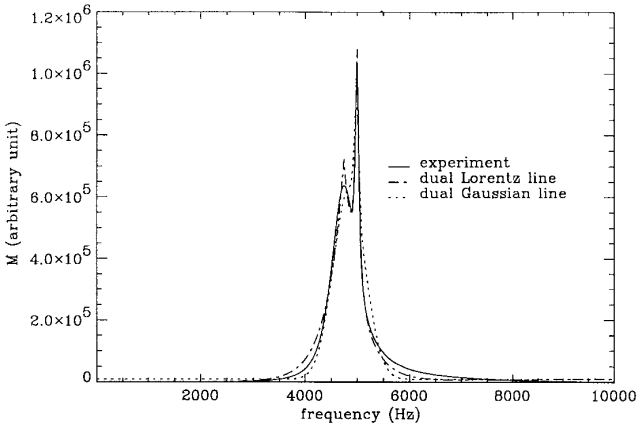

FIG. 4. The comparison of lineshape models: dual-Lorentzian and dual-Gaussian lines. The spectrum was measured at TE = 0.1 ms for the water-saturated sample with a wide fracture.

TABLE 1
Lineshape Characteristics of Water-Saturated Samples

Sample	$\delta\omega_m/2\pi$ (Hz)	$\delta\omega_f/2\pi$ (Hz)	$(\omega_{0f} - \omega_{0m})/2\pi$ (Hz)
A (wide)	324	49	255
B (middle width)	315	125	253
C (narrow)	308	93	265
D (no fracture)	330		

The response using oil as the saturating liquid was also investigated. The same samples were dried and resaturated with hexadecane. The spectra obtained from oil-saturated samples are shown in Figs. 3A–3D. Generally speaking, we observed very similar patterns for the oil-saturated cases as for the water-saturated cases. These results indicate that although surface relaxation between oil and rock is expected to be weaker than that between water and rock, the liquid/solid surface interactions are sufficiently strong so that the relaxation rate in the porous matrix is much faster than that in the fracture for either oil or water saturation.

Lineshape analysis was performed with these data using nonlinear regression with the dual-peak models described in Eqs. [3] and [4] for Lorentzian and Gaussian lineshapes, respectively. Figure 4 shows the spectrum corresponding to TE = 0.1 ms for the sample corresponding to Fig. 1A with the results of the fitting performed with the two models. The Lorentzian lineshape model appears to provide a better fit to the data than the Gaussian lineshape model. This seemed to be the case for all of the lineshape analyses in this study, although very precise fits are not to be expected with these simplified models. In particular, we found that the linewidth is represented relatively well by the Lorentzian model; the discrepancy between the experimental data and the lineshape model is primarily in the wings. Such discrepancy is typical for inhomogeneously broadened lines (*7*).

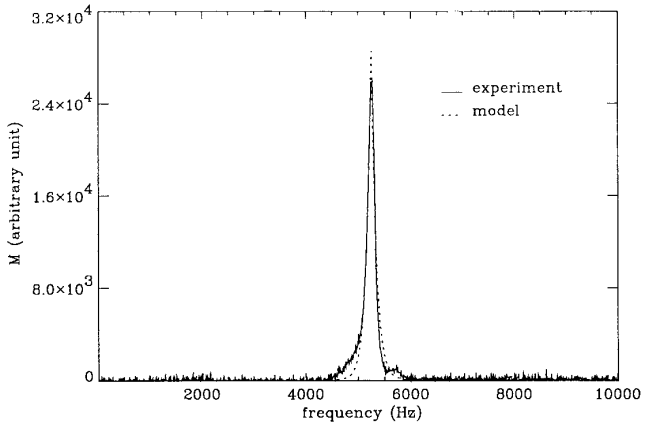

FIG. 5. Single-Lorentzian line nonlinear-least-squares fitting to the spectrum of a water-saturated sample with a wide fracture (TE = 200 ms).

TABLE 2
Lineshape Characteristics of Oil-Saturated Samples

Sample	$\delta\omega_m/2\pi$ (Hz)	$\delta\omega_f/2\pi$ (Hz)	$(\omega_{0f} - \omega_{0m})/2\pi$ (Hz)
A (wide)	327	103	256
B (middle width)	322	108	264
C (narrow)	320	205	265
D (no fracture)	321		

The lineshape characteristics of the two peaks analyzed using the dual-Lorentzian model (the fractured cases) or single-Lorentzian model (the nonfractured case) are shown in Table 1. These results were obtained by analyzing the spectra corresponding to the shortest TE value (0.1 ms). For Samples B and C, because of significant overlapping of the two parts of the spectra, a modified approach was used. We first analyzed a spectrum corresponding to a long TE value, which represents fracture only, with the single-Lorentzian line model (Fig. 5), for obtaining the parameters ω_{0f} and $\delta\omega_f$. Assuming the lineshape is independent of TE for the fracture, while the magnitude is TE dependent, we used these ω_{0f} and $\delta\omega_f$ values as known parameters in the dual-Lorentzian line model to obtain the rest of the parameters. Note that the values of $\delta\omega/2\pi$ calculated from the Lorentzian model represent half-linewidth values of the corresponding peaks. Oil-saturated samples give results similar to those of the water-saturated cases, and the results are shown in Table 2.

From the two tables, we see that the values of $\delta\omega_m/2\pi$ vary little among the samples, which is expected since they correspond to the fluid in the porous matrix. Values of $\delta\omega_f/2\pi$ are smaller for the sample with a broad fracture, but larger for the sample with a narrow fracture. The behavior of water-saturated sample B is somewhat irregular. The irregularity can be traced back from the peculiar lineshape acquired with longer TE values (see Fig. 1C). Experiments were repeated for another set of Leuters limestone samples and a set of Calico limestone samples which did not exhibit such strange behavior. Further analysis is necessary for the mechanism responsible for the lineshape in sample B. The similarity of values of $(\omega_{0f} - \omega_{0m})/2\pi$ in samples with different fracture widths suggests that fluids in fractures shift insignificantly from the bulk fluid resonance frequencies. Thus, the values of $(\omega_{0f} - \omega_{0m})/2\pi$ represent primarily the shift due to porous matrix.

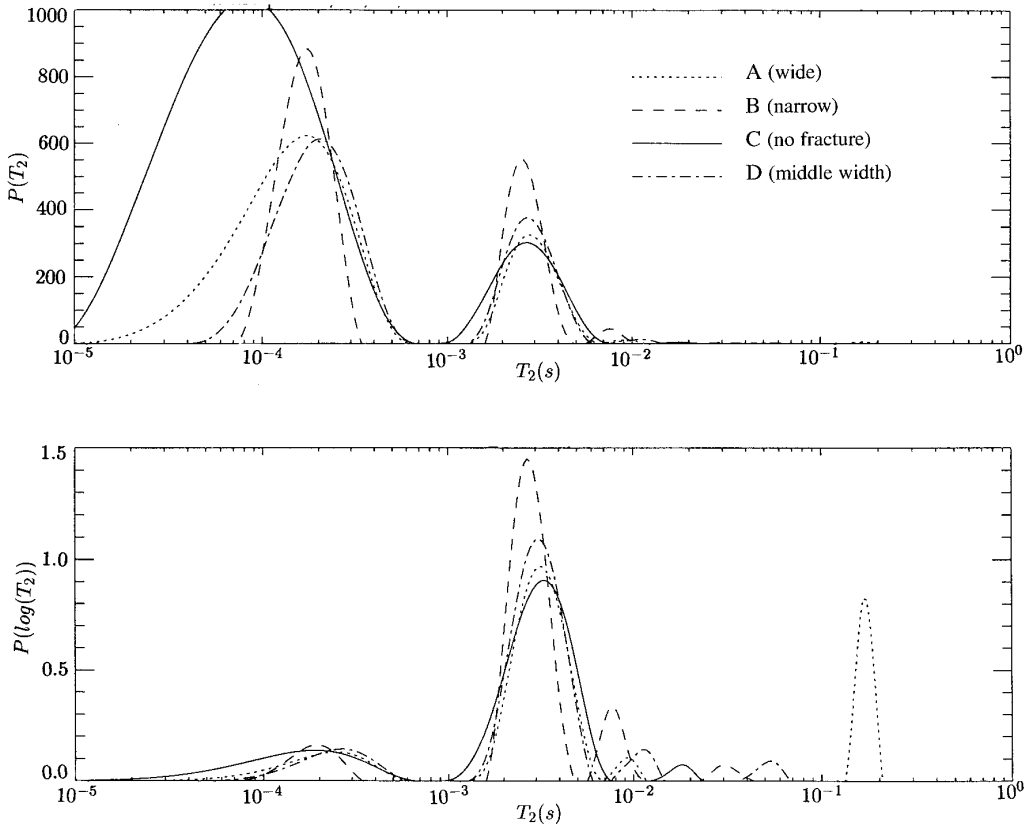

FIG. 6. T_2 distribution for water-saturated samples.

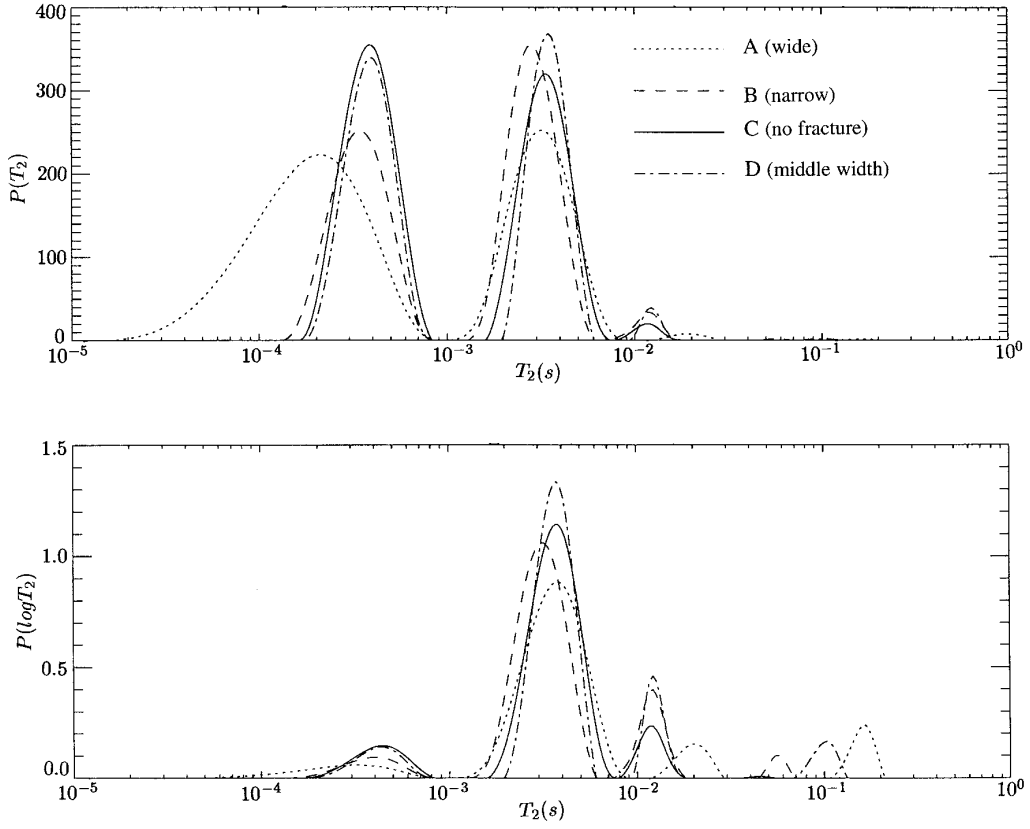

FIG. 7. T_2 distribution for oil-saturated samples.

T_2 Analysis

The measured magnetization decays corresponding to the TE values ranging from 0.1 to 200 ms for each of the water-saturated samples were used to estimate the corresponding T_2 distributions (*6*). The distribution function $P(T_2)$ is plotted in the first graph in Fig. 6. In the second graph, $P[\log(T_2)]$ is plotted to represent a histogram of the distribution curve in the semilog scale; thus $P[\log(T_2)]$-$d[\log(T_2)]$ is directly proportional to the relative amount of fluid in the corresponding interval $d[\log(T_2)]$ (*6*). Below approximately 10^{-2} s, the relaxation distributions are similar, indicating similar pore structures within the porous matrix regions. The distribution curves differ significantly at longer relaxation times where a small peak, evidently representing the fluid in the fracture, is observed.

The location of the peak corresponding to the greatest relaxation time is consistent with the width of fracture: the wider the fracture, the larger the corresponding value of T_2. The peak with the second largest T_2 may also be representing a small number of large pores. The oil-saturated samples exhibit similar trends, as shown in Fig. 7. The values of the relaxation times corresponding to the peaks with the largest T_2 have a similar dependence on fracture width, although the difference in T_2 values among those samples are somewhat smaller than that in the water-saturated cases. This result is quite reasonable in view of the fact that the surface relaxation rate is lower for oil-saturated systems than for water-saturated systems. Thus, the second term in Eq. [7] tends to be less dominant.

DISCUSSION

A disadvantage of using the Hahn spin-echo sequence for T_2 measurements is that the magnetization decay may be affected by diffusion under the internal gradient. That effect is proportional to (*7*)

$$\exp\left[-D\left(\gamma\frac{\partial H}{\partial z}\right)^2\frac{\mathrm{TE}^3}{12}\right]. \qquad [10]$$

Clearly, this term will have a greater effect with longer TE because of the TE^3 dependence. Both commercially available tools (*8, 9*) use the CPMG technique, so this problem can be minimized. The lack of knowledge of the internal gradient will not affect the qualitative features of the approach presented in this paper. However, the accuracy in the estimation of the long T_2 component could be affected in our analysis. Examining the intensities of the longest-relaxation-

time peaks in Figs. 6 and 7, we see that the amounts of fluid corresponding to the peaks with the largest T_2 for the different fractured samples are not profoundly different. We believe part of the reason may be explained by the extra decay term described in Eq. [10].

On the other hand, the lineshape analysis can be performed on the data obtained at very short TE for which both the relaxation and the diffusion effects can be ignored. The disadvantage of the lineshape method is that it requires a relatively homogeneous static magnetic field. This is not a great problem for laboratory analysis but is not suitable for those logging tools which are operating in a nonuniform static field. However, future hardware improvements can certainly make the technique feasible.

The utility of lineshape analysis for systems with very broad lines needs to be evaluated. The combination of lineshape analysis and T_2 weighting could provide more reliable measurements for fracture detection in broad-line systems. The T_2 distribution analysis is presumably independent of lineshape. However, its sensitivity is limited by the amount of fluid in the fractures and the contrast in relaxation times between the fluid in the different regions. The lineshape technique requires a homogeneous static field, which may require hardware modification or reduction of the sensitive volume in the current tools in order to take advantage of the peak separation between fluids in fractures and on porous matrix.

SUMMARY

We have presented experimental data which demonstrate the use of NMR lineshape and relaxation analyses for characterizing fractures and fluid distributions in those media. The results show that NMR spectroscopic techniques have a great potential for fracture characterization. We demonstrated that the lineshape analysis could provide information about the porous media structures. Due to the simplicity of the technique, it could be useful with hardware and software modifications in the logging tools.

REFERENCES

1. R. L. Kleinberg, *in* ''Encyclopedia of Nuclear Magnetic Resonance'' (D. M. Grant and R. K. Harris, Eds.), Vol. 8, p. 4960, Wiley, Chichester, 1996.
2. S. Chen, X. Yao, J. Qiao, and A. T. Watson, *Magn. Reson. Imaging* **13**(4), 599 (1995).
3. P. D. Majors, P. Li, and E. J. Peters, 1995. [Paper SPE 30557, presented at annual Soc. Petrol. Eng., Dallas, Oct. 1995]
4. C. H. Durney, J. Bertolina, D. C. Ailion, R. Christman, A. G. Cutillo, A. H. Morris, and S. Hashemi, *J. Magn. Reson.* **85,** 554 (1989).
5. K. R. Brownstein, and C. E. Tarr, *Phys. Rev. A* **19,** 2446 (1979).
6. H.-K. Liaw, R. Kulkarni, S. Chen, and A. T. Watson, *AIChE J.* **42,** 538 (1996).
7. C. P. Slichter, ''Principles of Magnetic Resonance,'' Springer-Verlag, New York, 1990.
8. S. Stricman, ''Nuclear Magnetic Resonance Sensing Apparatus and Techniques,'' U.S. Patent 4,710,713, 1987.
9. R. L. Kleinberg, A. Sezginer, D. D. Griffin, and M. Fikuhara, *J. Magn. Reson.* **97,** 466 (1992).